193165
30 P

NASA Contractor Report 191543

ICASE Report No. 93-74

ICASE

20 Years of Excellence

COMPUTATION OF THE SOUND GENERATED BY ISOTROPIC TURBULENCE

S. Sarkar

M. Y. Hussaini

NASA Contract No. NAS1-19480
October 1993

Institute for Computer Applications in Science and Engineering
NASA Langley Research Center
Hampton, Virginia 23681-0001

Operated by the Universities Space Research Association

National Aeronautics and
Space Administration

Langley Research Center
Hampton, Virginia 23681-0001

ICASE Fluid Mechanics

Due to increasing research being conducted at ICASE in the field of fluid mechanics, future ICASE reports in this area of research will be printed with a green cover. Applied and numerical mathematics reports will have the familiar blue cover, while computer science reports will have yellow covers. In all other aspects the reports will remain the same; in particular, they will continue to be submitted to the appropriate journals or conferences for formal publication.

COMPUTATION OF THE SOUND GENERATED BY ISOTROPIC TURBULENCE

S. Sarkar[1]
Department of Applied Mechanics and Engineering Sciences
University of California at San Diego

M. Y. Hussaini[1]
Institute for Computer Applications in Science and Engineering
NASA Langley Research Center

ABSTRACT

The acoustic radiation from isotropic turbulence is computed numerically. A hybrid direct numerical simulation approach which combines direct numerical simulation (DNS) of the turbulent flow with the Lighthill acoustic analogy is utilized. It is demonstrated that the hybrid DNS method is a feasible approach to the computation of sound generated by turbulent flows. The acoustic efficiency in the simulation of isotropic turbulence appears to be substantially less than that in subsonic jet experiments. The dominant frequency of the computed acoustic pressure is found to be somewhat larger than the dominant frequency of the energy-containing scales of motion. The acoustic power in the simulations is proportional to ϵM_t^5 where ϵ is the turbulent dissipation rate and M_t is the turbulent Mach number. This is in agreement with the analytical result of Proudman (1952), but the constant of proportionality is smaller than the analytical result. Two different methods of computing the acoustic power from the DNS data bases yielded consistent results.

[1]This research was supported by the National Aeronautics and Space Administration under NASA Contract No. NAS1-19480 while the authors were in residence at the Institute for Computer Applications in Science and Engineering (ICASE), NASA Langley Research Center, Hampton, VA 24681.

Introduction

In 1952, Lighthill posed the problem of estimating the sound radiated by "a fluctuating fluid flow occupying a limited part of a very large volume of fluid of which the remainder is at rest" - the fluid flow of course is either ordered, with coherent distributions of vorticity, or disordered and turbulent. It is only now, four decades later, that the simplest possible model of this problem i.e., sound radiated from a limited body of isotropic turbulence bounded by a quiescent fluid, is amenable to numerical simulation.

Isotropic turbulence in a bounded domain is a model wherein the turbulence is unaffected by the boundaries enclosing the fluid, and furthermore the statistical moments are spatially invariant and independent of orientation. Isotropic grid turbulence is a similar idealization, in that the turbulence is enclosed by wind tunnel walls and the homogeneity of the turbulence in the central region is known to be unaffected by the wall boundary layers. The problem of sound emitted by isotropic turbulence has been investigated by Proudman (1952), and more recently by Lilley (1993) in an analytical study and by Witkowska and Juve (1993) in a large eddy simulation (LES). The isotropic turbulence is represented in our numerical study by a periodic box which contains the fluid motion and is surrounded by a layer in which the velocities decrease to zero. The fluid motion inside the periodic box is simulated, and it is assumed that the sound radiated by the periodic box is unaffected by the surrounding thin layer.

Two possible numerical approaches to the prediction of sound produced by turbulence are the direct numerical simulation (DNS) and the hybrid DNS. In a DNS, all relevant scales of motion are numerically resolved in a solution of the compressible Navier-Stokes equations; while in a hybrid DNS only the turbulent flow is resolved numerically. Sarkar and Hussaini (1993) have estimated the turbulence Reynolds numbers Re_t that could be obtained for a three-dimensional calculation of sound generated by turbulence with the two methods for a given spatial grid. It was found that for $M_t = 0.01$ and 0.1, the Re_t that can be simulated by DNS of sound on a uniform grid is respectively 0.004 and 0.08 times smaller than that achieved in the hybrid DNS method. Evidently, the much larger computational volume required in the DNS of sound approach leads to a much lower turbulence Reynolds number relative to the hybrid approach. By stretching the

computational grid or by using overlapping grids, the Re_t obtainable with the DNS of sound approach can be increased. However, the effect of grid stretching on the accuracy of the far-field acoustic pressure which is several orders of magnitude smaller than the aerodynamic pressure has to be carefully examined. Crighton (1993) points out that computations of low Mach number aeroacoustics by the DNS of sound approach have to contend with a number of difficulties which include the large disparity between the acoustic length scale and the turbulence integral length scale, the much smaller energy in the acoustic far field relative to the turbulent energy, and the multipole structure of the basic acoustic source. Due to these reasons, Lighthill (1993) recommends the use of an acoustic analogy for the computation of sound radiated from low Mach number flows. The present work employs the the hybrid DNS approach with the Lighthill acoustic analogy for the purpose of computing the sound generated by three-dimensional, fully turbulent flow. Lighthill's analogy has been used previously to compute the sound numerically from the large-scale instability waves in a shear layer by Gatski (1979), but we are not aware of any previous attempt to use the analogy within the framework of three-dimensional DNS of turbulence.

The acoustic analogy which was first proposed by Lighthill (1952) reduces the aeroacoustics problem to an inhomogeneous wave equation. In his analogy, Lighthill chose the homogeneous part to be a linear wave equation for the density and obtained the acoustic far-field as an integral of the equivalent acoustic sources in a uniform medium at rest which replace the fluid motion inside a bounded volume. Furthermore, by considering the statistics of the acoustic sources, Lighthill deduced the eighth-power law at low Mach numbers for the net acoustic power radiated from a turbulent region.

Lighthill's analogy was followed by other analogies (Phillips (1960), Powell (1964), Ribner (1964), Lilley (1974), and Howe (1975)). In the analogies of Phillips, Lilley and Howe, the homogeneous part of the equation for the acoustic variable is a nonlinear convected wave equation rather than the linear wave equation in Lighthill's analogy, and as discussed by Goldstein (1974), Crighton (1975) and Ffowcs Williams (1977) has the advantage of explicit consideration of the convection and refraction of sound by turbulence. Powell and Howe rewrite the term $\mathbf{u}\cdot\nabla\mathbf{u}$ as $\boldsymbol{\omega}\times\mathbf{u}+\nabla\mathbf{u}^2/2$ in their analogies

which leads to an explicit vorticity-dependent term in the inhomogeneous part of the wave equation. The explicit appearance of the vorticity in the forcing term is convenient in unsteady flows such as the Von Karman vortex shedding in the laminar wake of a cylinder, but perhaps not so important in high Reynolds number turbulent flows where the flow is more incoherent and cannot be idealized as a simple collection of idealized vortices. It is also more convenient in the context of vortex methods (Leonard (1985)). Applications of the Lighthill theory are consistent with experimental data on noise radiated from subsonic jets running at ambient temperatures. However in supersonic jets (Seiner(1992)), it may be necessary to account for additional physical features explicitly such as Mach wave radiation, jet screech, and other shock-associated noise. In our work on noise generated from isotropic turbulence at low Mach numbers, Lighthill's acoustic analogy is the preferred representation and is the one followed herein.

Computation of the Lighthill acoustic analogy

The acoustic analogy of Lighthill can be written in the space - derivative form

$$p_A(\mathbf{x},t) = \frac{1}{4\pi}\int \frac{T_{ij,ij}(\mathbf{y},t-r/c_0)}{r}\,d\mathbf{y}, \tag{1}$$

but for a far-field location of the observer point with $|x| >> |y|$, Lighthill showed that the integrand in (1) can be approximated by the second time derivative taken at the retarded time yielding

$$p_A(\mathbf{x},t) = \frac{1}{4\pi c_0^2}\frac{x_i x_j}{x^3}\int \ddot{T}_{ij}(\mathbf{y},t-r/c_0)\,d\mathbf{y}, \tag{2}$$

where p_A is the fluctuation of pressure relative to the ambient, c_0 is the ambient speed of sound, and $r = |\mathbf{x}-\mathbf{y}|$. In Eq. (1), density fluctuations are neglected in the source term and the approximation, $T_{ij,ij} \simeq \partial^2(\bar{\rho}u_i u_j)/\partial y_i \partial y_j$, is utilized since only low Mach numbers are considered in the present work. Here, $\bar{\rho}$ is the mean density which is of course a constant equal to the ambient density of the surrounding medium which is at rest. In Eq. (2), $\ddot{T}_{ij}(\mathbf{y},t-r/c_0)$ denotes $\partial^2(\bar{\rho}u_i u_j)/\partial t^2$ evaluated at retarded time $t-r/c_0$.

The major advantage of the time-derivative form of the acoustic analogy over the space-derivative form is that the quadrupole nature of the sound source is directly evident

in Eq. (2) but not in Eq. (1). However, the computer storage requirements of the space-derivative form is smaller by a factor of 6 relative to those of the time-derivative form which could present a significant advantage in large-scale computations where computer memory is a constraint. In Sarkar and Hussaini (1993), the relative advantages of Eqs. (1) and (2) were investigated for a test problem with an imposed quadrupole. The retarded time effect was accounted for by the time accumulation method wherein the observer time t was approximated by $t \simeq [(\tau + c_0 r)/\Delta t]\Delta t$ where [.] denotes the integer value function, and Δt denotes the time step used for time advancement of the flow. It was found that the number of time points required for the spatial derivative form is too large; turbulence of the quadrupole source type requires $O(1/M_t^2)$ time points per oscillation of the source. Due to the stringency of this requirement, we choose the time-derivative form, Eq. (2), over the space-derivative form, Eq. (1).

Furthermore, Eq. (1) is not quite appropriate here because of the periodic boundary conditions used for the turbulence simulation. Because of the non-zero velocity at the fluid boundary of the periodic box, the dipole contribution to the sound from the surface of the flow domain is non-zero and would be included in a calculation using Eq. (1). The surface contribution is an artifact of the boundary conditions and is not of interest to us. Eq. (2), on the other hand, gives directly the quadrupole sound characteristic of a finite volume of turbulent flow embedded in a medium at rest. We ensure that the periodic boundary conditions do not unrealistically affect *both* the flow field and acoustic source by keeping the length of the computational domain much larger than the spatial correlation lengths of the velocity field u_i and the acoustic source $\ddot{T}_{ij}$.

In the case of unforced isotropic turbulence, the acoustic source term, $\int \ddot{T}_{ij}(\mathbf{y}, t - r/c_0)\, d\mathbf{y}$, decays in time. Consequently, the acoustic pressure is statistically unsteady and time averaging is inappropriate for statistical analysis. Short-time averaging was used in Sarkar and Hussaini (1993) to compute the statistics of the acoustic pressure. But such a method has since proven to be unsatisfactory due to the time scale of the turbulence decay being of the same order as the time scale of the acoustic fluctuations. The results presented here are substantially different from the preliminary work of Sarkar and Hussaini (1993). In the present work, ensemble averages are used to compute the acoustic intensity, power

and frequency spectrum. 20 cases were run with the same parameters and the same initial statistics, but with different instantaneous initial conditions. For each case, the observation points were distributed on two concentric spheres in the far-field, 10 on each sphere. Due to the isotropy of the turbulence, the 20 different simulations with 10 different observer points at the same distance from the center of the flow domain lead to 200 different samples of the acoustic pressure which is a sufficiently large number to obtain acceptable statistics. The scaled acoustic power is obtained by averaging over 400 samples.

Flow simulation method

The turbulent flow inside a cubical domain is obtained by solving the compressible Navier-Stokes equations by a numerical algorithm which was originally developed to investigate compressibility effects in isotropic turbulence (Erlebacher, Hussaini, Kreiss, and Sarkar (1990), Sarkar, Erlebacher, Hussaini, and Kreiss (1991a)), and homogeneous shear turbulence (Sarkar, Erlebacher, and Hussaini(1991b), Sarkar (1992)). The homogeneous turbulence problem permits periodic boundary conditions in all three coordinate directions. It is of course necessary that the length of the computational domain be much larger than the integral length scale of the turbulence for obtaining realistic flow fields. Spectral accuracy is obtained by using a Fourier collocation method for the spatial discretization of the governing equations. A third order, low storage Runge-Kutta scheme is used for advancing the solution in time.

Initial conditions have to be prescribed for u_i', ρ, p and T. The initial velocity field is split into two independent components, that is, $u_i' = u_i^{I'} + u_i^{C'}$, where each component has a zero average. The solenoidal velocity field $u_i^{I'}$ which satisfies $\nabla.\mathbf{u}^{I'} = 0$ is chosen to be a random Gaussian field with the power spectrum

$$E(k) = k^4 \exp(-2k^2/k_m^2) \tag{3}$$

where k_m denotes the wave number corresponding to the peak of the power spectrum. The compressible velocity $u_i^{C'}$ which satisfies $\nabla \times \mathbf{u}^{C'} = 0$ is also chosen to be a random Gaussian field satisfying the same power spectrum, Eq. (3). The power spectra of the

two velocity components are scaled so as to obtain a prescribed $u_{\rm rms} = \sqrt{\overline{u_i' u_i'}}$, and a prescribed $\chi = u^C_{\rm rms}/u_{\rm rms}$ which is the compressible fraction of kinetic energy. The pressure $p^{I'}$ associated with the incompressible velocity is evaluated from the Poisson equation

$$\nabla^2 p^{I'} = -\bar{\rho} u^{I'}_{i,j} u^{I'}_{j,i}. \tag{4}$$

It remains to specify the initial values of the thermodynamic variables. The mean density $\bar{\rho}$ is chosen equal to unity, and $\bar{p}$ is chosen so as to obtain a prescribed Mach number $u_{\rm rms}/\sqrt{\gamma \bar{p}/\bar{\rho}}$ characterizing the turbulence. The fluctuating density ρ' and compressible pressure $p^{C'}$ are chosen as random fields with the power spectrum determined by Eq. (3) and prescribed $\rho_{\rm rms}$ and $p^C_{\rm rms}$. The pressure then becomes $p = \bar{p} + p^{I'} + p^{C'}$, the density is $\rho = \bar{\rho} + \rho'$, and the instantaneous temperature T is obtained from the equation of state $p = \rho R T$. We note that the splitting of velocity and pressure into incompressible and compressible components is confined to the specification of initial conditions. No such split is carried out while computing the acoustic sources during the time evolution. Although the numerical algorithm is capable of simulating compressible turbulence with non-zero density fluctuations and non-zero dilatation, we consider low Mach number, quasi-incompressible turbulence in the present paper. The acoustic source T_{ij} is approximated by $\bar{\rho} u_i u_j$ and density fluctuations neglected in the acoustic source.

Characteristics of the simulated turbulence

The acoustic radiation from isotropic turbulence has been computed with the hybrid DNS method for the case with the following initial parameters

$$Re_\lambda = 50, \quad , \quad M_t = 0.05$$

where Re_λ is the Taylor microscale Reynolds number, and M_t the turbulent Mach number.(Note that $Re_\lambda = q\lambda/\nu$ where $q = \sqrt{\overline{u_i' u_i'}}$, $\lambda = q/\sqrt{\overline{\omega_i' \omega_i'}}$, ω_i' is the fluctuating vorticity, and ν is the kinematic viscosity; while $M_t = q/\bar{c}$ where $\bar{c}$ is the mean speed of sound.) The initial energy spectrum is given by Eq. (3) with $k_m = 6$. The initial data for the case discussed here is chosen to be incompressible; the velocity is solenoidal

($\chi = 0$), the density is constant, and the pressure is initialized with the usual Poisson equation applicable to incompressible flows. Twenty simulations on a 64^3 grid with a time step of $\Delta t = 0.00275(K/\epsilon)_0$ were caried out. A single, higher-resolution simulation was performed on a 128^3 spatial grid with $\Delta t = 0.001375(K/\epsilon)_0$, other parameters remaining equal, to check the accuracy of the coarse-grid solution. The simulations were conducted for one eddy turnover time ($\epsilon_0 t/K_0 = 1$). The 64^3 simulations were used to obtain ensemble-averaged statistics from the instantaneous acoustic pressure, while the 128^3 simulation was used to obtain the acoustic power from the appropriate flow statistics.

The turbulence statistics at a given time in a DNS case are obtained by averaging over the computational volume. For example the turbulent kinetic energy $K =< u_i u_i > /2$ where $< . >$ denotes a volume average. In the present simulations, the turbulence is unforced. Consequently, the turbulent kinetic energy decays in time. Figs. 1 and 2 show the evolution of the turbulent kinetic energy K and turbulent dissipation rate ϵ, respectively. K decreases by about a factor of 5 by the end of the simulation. The evolution of K for $\epsilon_0 t/K_0 > 0.2$ is well represented by a power law decay $(t - t_0)^{-n}$ with the exponent $n = 1.4$, a value which is slightly larger than experimentally measured exponents which lie in the range $1.15 < n < 1.35$. The turbulent dissipation rate ϵ increases during the initial transient in Fig. 2 due to the generation of small-scale fluctuations, and finally decays in the absence of external forcing. The microscale Reynolds number Re_λ whose evolution is shown in Fig. 3 decays by a factor of 3 at the end of the simulation. The simulation is terminated at a nondimensional time $\epsilon_0 t/K_0 = 1$, because Re_λ at later times could become too small to represent realistically the spatio-temporal complexity of turbulence. The skewness of the velocity derivative $Sk = \overline{(\partial u/\partial x)^3}/[\overline{(\partial u/\partial x)^2}]^{3/2}$ is a measure of the non-linear vortex stretching. According to Lesieur(1990), experiments on grid turbulence give $Sk \simeq -0.4$, while simulations give $Sk \simeq -0.5$. Fig. 4 shows that skewness factor asymptotes to a value of $Sk = -0.46$ in the DNS which is consistent with previous experiments and simulations.

Characteristics of the computed acoustic pressure

The fluctuating acoustic pressure is computed from the DNS data by the temporal form of the Lighthill analogy,

$$p'_A(\mathbf{x},t) = \frac{1}{4\pi c_0^2}\frac{x_i x_j}{x^3}\int [\ddot{T}_{ij}] - \overline{[\ddot{T}_{ij}]}\, d\mathbf{y}. \tag{5}$$

where [.] denotes evaluation at retarded time, while the overbar denotes ensemble average. Thus, $p_A(\mathbf{x},t)$ is computed from Eq. (2); it's ensemble average calculated over the 20 DNS cases; and finally, the ensemble average is subtracted out to calculate $p'_A(\mathbf{x},t)$. Fig. 5 shows the evolution of the acoustic pressure fluctuation p'_A normalized by the ambient pressure P_0. The smallness of the acoustic pressure fluctuation which is about seven orders of magnitude smaller than the thermodynamic pressure would present a formidable challenge for the direct computation of sound by simulation of the compressible Navier-Stokes equations in the far-field. Since the turbulent source decays with time, the acoustic pressure also decays with time. We have tried to factor out the decay in turbulence statistics by dividing the random pressure signal $p'_A(t)$ by an appropriate deterministic function $g(t)$. The choice of $g(t)$ was guided by the analysis of Proudman (1952) who considered the generation of noise by isotropic turbulence and used statistical models of various two-point moments within the framework of the Lighthill analogy to obtain the following expression for the acoustic power P_A per unit mass

$$P_A = \alpha(u^3/l)\frac{u^5}{c_0^5} \tag{6}$$

where α is a constant related to the shape of the longitudinal velocity correlation $f(r)$, u is the root mean square (rms) of one of the velocity components, and l is the longitudinal integral length scale of the velocity. For the Heisenberg form of the energy spectrum, Proudman obtains

$$P_A = 38(u^3/l)\frac{u^5}{c_0^5} \tag{7}$$

and, with the assumption $f(r) = e^{-\pi(r/l)^2/4}$, Proudman obtains

$$P_A = 13(u^3/l)\frac{u^5}{c_0^5} \tag{8}$$

Eq. (8) implies that $g(t) \propto \sqrt{\epsilon M_t^5}$ can be used to normalize the acoustic pressure p_A in order to factor out the temporal decay. Fig. 6 shows the evolution of rescaled acoustic pressure p_A^* defined by

$$p_A^* = \frac{(p'_A)(x/L)}{\sqrt{(\epsilon L/c_0^3)M_t^5}}$$

Here, L is the length of the computational region. It appears that the normalization does factor out the temporal decay of the acoustic pressure. Fig. 7 shows the acoustic pressure fluctuations at different observer points. The instantaneous pressure signal at a given observation point is non-periodic, chaotic, and has a range of frequencies.

The rms acoustic pressure $p_{\rm rms}(t)$ observed at a distance x is obtained by ensemble-averaging over 200 samples of fluctuating acoustic pressure p'_A. These samples are obtained from the 20 cases in the DNS with each case having 10 observation points per sphere distributed on two concentric spheres around the center of the flow domain. The acoustic power emitted from the volume V of fluid is

$$P_V(t) = \frac{p_{\rm rms}^2(t)}{\rho_0 c_0} 4\pi r^2$$

and the acoustic power per unit mass of turbulent fluid is

$$P_A(t) = \frac{P_V(t)}{\rho_0 V}. \tag{9}$$

Fig. 8 shows the acoustic power in decibels from the DNS and the theoretical result. The dotted curve in Fig. 8 corresponds to a value of $\alpha = 13$ in Proudman's work giving

$$\begin{aligned} P_A &= 8.7\epsilon(t)\frac{u(t)^5}{c^5} \\ &= 0.5\epsilon(t)M_t(t)^5 \end{aligned} \tag{10}$$

and is obtained from Eq. (8) by using the definition of $M_t = \sqrt{2K}/c_0$ and our DNS result $\epsilon \simeq 1.5u^3/l$. The computed power is smaller than that obtained from Eq. (10) by $6-8$ dB over the time of the simulation. The ratio $P_A/\epsilon M_t^5$ varies between 0.15 and 0.07 in Fig. 9, i.e., by a factor of 2 during the decay of turbulent kinetic energy, while the numerator and denominator vary by about a factor of 15 during that time. Thus, the DNS is consistent with Proudman's result that P_A is proportional to ϵM_t^5. However,

if the proportionality constant from the DNS is taken to be $P_A/\epsilon M_t^5 \simeq 0.10$, it is smaller relative to Proudman's result, Eq. (10), by a factor of 5.

Witkowska and Juve (1993) have computed the sound generated from unforced isotropic turbulence by performing large eddy simulations (LES) on 16^3 spatial grids for determining the turbulent flow and then using the Lighthill acoustic analogy for computing the far-field sound. Five turbulent Mach numbers in the range of 0.012 to 0.015 were considered; the initial Re_λ was about 400. In agreement with our DNS results, the LES study finds that, although the acoustic power is proportional to ϵM_t^5, it is 12 dB less than Proudman's result for the Heisenberg spectrum. According to Witkowska and Juve (1993), a reconsideration of Proudman's analysis with the von Karman spectrum instead of the Heisenberg spectrum decreases the theoretical estimate so that the LES result is 6dB lower than the revised theoretical result.

The turbulence in the DNS has moderate to low Reynolds number since Re_λ decays from a value of 50 to 15 during the simulations. The LES of Witkowska and Juve (1993) has a turbulence Reynolds number which is a factor of 10 higher than the DNS, albeit with the approximations inherent in a subgrid scale model. Although, there is a difference in Reynolds number, the DNS and LES studies are consistent in giving an acoustic power which is a factor of 5 smaller than Proudman's result Eq. (10). Proudman's analysis predates the present computational studies by about four decades and, of necessity, had to employ various assumptions such as Gaussian statistics for the velocity and its time derivatives, neglect of retarded time during evaluation of the integral expression for the acoustic power, neglect of the decay of unforced isotropic turbulence, and a specific shape for the longitudinal space correlation $f(r)$. Lilley (1993), in a reconsideration of Proudman's analysis, finds that the coefficient α in Eq. (6) is likely to be between 3 and 10. In contrast, our DNS gives $\alpha \simeq 2.6$. The analysis of Lilley (1993) also elegantly shows that the acoustic power is sensitive to the shape of the space-time covariance of T_{xx}, the flatness factor of the velocity, and is proportional to the fourth power of the characteristic Strouhal number $s = \omega l/u$ where l and ω are the integral scales associated with the spatial and temporal autocorrelations of the velocity, respectively, and u is the rms of a velocity component. Using the velocity flatness factor of 3.0 in our DNS results,

Lilley (1993) finds $\alpha = 3.4$ with $s = 1$ and $\alpha = 8.3$ with $s = 1.25$ in an analytical calculation which assumes the same $f(r/l)$ that corresponds to Proudman's $\alpha = 13$. Given the sensitvity of α to the assumed model correlations, it is not surprising that the analytically determined values for α are somewhat different from the corresponding results in the simulations. Overall, the DNS value of α is consistent with the lower end of the range of values of α found by Lilley (1993).

The scaled acoustic power $P_A/\epsilon M_t^5$ is significantly smaller than that typical of subsonic jets. In subsonic jets the acoustic efficiency (sound power/jet power) according to Lighthill (1954) is approximately $10^{-4}M^5$, where M is the jet Mach number. The turbulence intensity u_{rms}/U_{jet} can be roughly estimated to be 0.17, and ϵ is roughly 0.1 of the jet power, which implies that $P_A/\epsilon M_t^5 \simeq 7$. Thus the sound radiated from isotropic, homogeneous turbulence is significantly smaller than that typical of jet acoustics. We argue below that one of the reasons for this dissimilarity is the homogeneity constraint.

The acoustic pressure fluctuation is given by Eq.(5). Consider the integral in Eq. (5) as $M_t \to 0$.

$$\begin{aligned} & \int [\ddot{T}_{ij}] - \overline{[\ddot{T}_{ij}]}\, d\mathbf{y} \\ \to & \int \ddot{T}_{ij} - \overline{\ddot{T}_{ij}}\, d\mathbf{y} \\ = & \; V < \ddot{T}_{ij} > - V\overline{< \ddot{T}_{ij} >}. \end{aligned} \tag{11}$$

The second line in Eq. (11) follows because retarded time can be neglected in the limit of $M_t \to 0$, and the third line follows from the definition of the volume average denoted by $< . >$. In the case of homogeneous turbulence, $< \ddot{T}_{ij} >$ is equivalent to an ensemble average, and since further time averaging does not change a quantity which is already an average $\overline{< \ddot{T}_{ij} >} =< \ddot{T}_{ij} >$. Consequently the integral in Eq. (5) is zero when retarded time effects are neglected in the limit of $M_t \to 0$. However, in the case of inhomogeneous turbulence $< \ddot{T}_{ij} >$ is not a temporally smooth quantity, and this integral is not necessarily zero even if retarded time effects were neglected.

For small but finite Mach number, when retarded time effects cannot be neglected, it is clear that the volume integration smoothes out the temporal oscillation in $[\ddot{T}_{ij}]$ to a

greater extent in homogeneous turbulence than in inhomogeneous turbulence, which thus causes smaller fluctuations in the radiated sound from homogeneous turbulence relative to the inhomogeneous case.

The frequency content of the acoustic pressure was obtained by analyzing the normalized acoustic pressure $p_A^*(t)$ in Fourier space. The power spectrum $E_p(\omega)$ obtained by averaging over 400 records of $p_A^*(t)$ is shown in Fig. 10. The frequency is normalized by l_0/u_0, where l_0 is the initial longitudinal integral length scale and u_0 is the initial rms of a velocity component. The power spectrum in Fig. 10 has a peak at a Strouhal number $St = \omega l_0/u_0 \simeq 3.5$. Thus, the dominant frequency of the sound radiated to the far-field in the isotropic turbulence DNS is somewhat larger than the dominant frequency u_0/l_0 of the energy-containing range of turbulence.

Computation of the acoustic power from the turbulence statistics

The acoustic power obtained in our simulations is somewhat smaller than predicted by Proudman's analysis. This discrepancy motivated an alternative method to obtain the acoustic power wherein the the fourth-order, two-point correlation $\overline{\ddot{T}'_{xx}(0)\ddot{T}'_{xx}(r)}$ from the DNS is used.

Consider an observer point at location (x,0,0). Then, due to Eq. (5) for the acoustic pressure fluctuation, the acoustic power P_A per unit mass at the observer point given by Eq. (9) becomes

$$P_A(t) = \frac{1}{4\pi V c_0^5} \int\int \overline{\ddot{T}'_{xx}(\mathbf{x}_A, t_A)\ddot{T}'_{xx}(\mathbf{x}_B, t_B)}\, d\mathbf{x}_A d\mathbf{x}_B \tag{12}$$

where V is the source volume, and $\mathbf{x}_A$ and t_A denote the position of source point A and time of sound emission at point A so as to reach observer at time t; similarly, $\mathbf{x}_B$ and t_B refer to source point B. Proudman assumes that $\overline{\ddot{T}'_{xx}(\mathbf{x}_A, t)\ddot{T}'_{xx}(\mathbf{x}_B, t)}$ is constant over the maximum time difference $t_A - t_B$ so that retarded time effects can be ignored during the volume integration with respect to source point B. This assumption leads to

$$P_A(t) = \frac{1}{4\pi c_0^5} \int \overline{\ddot{T}'_{xx}(\mathbf{x}_A, t_A)\ddot{T}'_{xx}(\mathbf{x}_B, t_A)}\, d\mathbf{x}_A \,. \tag{13}$$

Proudman, then assumes that t_A can be considered constant during the integration over source point A, to obtain finally

$$P_A(t) = \frac{1}{4\pi c_0^5} \int \overline{\ddot{T}'_{xx}(\mathbf{x}_A)\ddot{T}'_{xx}(\mathbf{x}_B)}\, d\mathbf{x}_A \tag{14}$$

The two-point spatial autocorrelation in Eq. (14) is a function of $r = |\mathbf{x}_A - \mathbf{x}_B|$ only, due to the turbulence isotropy. Let us define $a'_i = (u^2 - < u^2 >, v^2 - < v^2 >, w^2 - < w^2 >)$, and denote the spatial correlation $\overline{(\partial^2 a'_i/\partial t^2)_A (\partial^2 a'_j/\partial t^2)_B}$ by $Q_{ij}(\mathbf{r})$. The subscript $i = 1, 2, 3$ denotes the x, y, z components, respectively. Then, Eq. (14) becomes

$$P_A(t) = \frac{1}{4\pi c_0^5} \int Q_{11}(\mathbf{r}) d\mathbf{r} \tag{15}$$

The following expression for Q_{ij} can be written due to the isotropy constraint (e.g. see Hinze(1975))

$$Q_{ij}(r) = \overline{(\partial^2 u^2/\partial t^2)'^2} \left[\frac{F(r) - G(r)}{r^2} r_i r_j + G(r)\delta_{ij}\right]$$

where the fluctuation $(\partial^2 u^2/\partial t^2)' = \partial^2 u^2/\partial t^2 - < \partial^2 u^2/\partial t^2 >$, while $F(r)$ and $G(r)$ are the longitudinal and lateral correlation functions associated with Q_{ij} respectively. Thus,

$$Q_{11}(r) = \overline{(\partial^2 u^2/\partial t^2)'^2} \left[F(r)\cos^2(\theta) + G(r)\sin^2(\theta)\right]$$

where θ is the angle between $\mathbf{r}$ and the x axis. The volume integration in Eq. (15) with respect to the separation vector $\mathbf{r}$ is then performed using a spherical coordinate system to yield

$$P_A(t) = \frac{\overline{(\partial^2 u^2/\partial t^2)'^2}}{c_0^5} \int_0^R \frac{r^2}{3}(F(r) + 2G(r))dr\ . \tag{16}$$

Proudman (1952) uses the statistical theory of isotropic turbulence to model the correlations in Eq. (16); we, on the other hand, directly compute $\overline{(\partial^2 u^2/\partial t^2)'^2}$, $F(r)$ and $G(r)$ from the DNS data base.

The longitudinal correlation functions $F(r)$ associated with Q_{ij}, and $f(r)$ associated with the velocity field are shown in Fig. 11 at the time $\epsilon_0 t/K_0 = 0.7$. Evidently, the presence of the second time derivative leads to a much smaller correlation length of the acoustic source relative to the velocity. To confirm our results, a new simulation was performed with twice the resolution in both space and time. Fig. 12 shows that the

higher resolution 128^3 simulation gives a result for $F(r)$ which is similar to the coarse-grid simulation. The correlation length scale for the acoustic source is 0.10, while the integral, Taylor and Kolmogorov length scales are 0.58, 0.12, and 0.03, respectively. It thus appears that the correlation length of $\partial^2 u^2/\partial t^2$ in our simulation of isotropic turbulence is smaller than the turbulence integral length scale and larger than the dissipative length scale.

Eq. (16) was used to provide an alternative estimate of the acoustic power from the DNS. Fig. 13 shows that the result from Eq. (16) is consistent with the previous result obtained from statistical post-processing of the instantaneous acoustic pressure. Since retarded times are neglected in simplifying the exact expression for the acoustic power Eq.(12) to obtain Eq. (16), it is not surprising that there is some difference between the two methods.

Conclusions

We have applied the hybrid DNS approach to the problem of sound generated by isotropic turbulence. The combination of a spectral DNS of isotropic turbulence and the Lighthill acoustic analogy is demonstrated to be a feasible approach for obtaining the instantaneous acoustic pressure. Although the time derivative form of the Lighthill acoustic analogy requires more computer memory for storage than the spatial derivative form, it is preferable due to a less stringent time step constraint.

The numerically computed acoustic efficiency of isotropic turbulence is much smaller than that in subsonic jet experiments. The frequency spectrum of the acoustic pressure indicates that the dominant acoustic frequency is somewhat larger than the frequency of the energy-containing eddies as found in Proudman (1952) and Lilley (1993). The computed acoustic power agrees with the theoretically derived proportionality to ϵM_t^5 deduced by Proudman (1952); however the constant of proportionality is smaller than the analytical result. The acoustic power was computed from the DNS both by ensemble-averaging the instantaneous acoustic pressure, and also from the two-point, fourth-order correlation $\overline{\ddot{T}'_{xx}(0)\ddot{T}'_{xx}(x)}$. The two methods for obtaining the acoustic power yield consistent results.

Proudman (1952) analytically obtained the following relation for the acoustic power,

$$P_A = \alpha(u^3/l)\frac{u^5}{c^5}$$

where $\alpha = 13$ with the particular choice $f(r) = e^{-\pi(r/l)^2/4}$ for the longitudinal velocity correlation. In contrast, $\alpha \simeq 2.6$ in the present DNS. The analysis of Lilley (1993) indicates that α is likely to have a value between 3 and 10. The analytical studies have had to necessarily make some assumptions about the space-time statistics of the acoustic source while the DNS, although free from such assumptions, is restricted to a moderate to small turbulence Reynolds number. The LES study of Witkowska and Juve (1993) which have turbulence Reynolds numbers larger than those in the DNS by an order of magnitude give $\alpha \simeq 2.5$. Although, the DNS and LES studies give consistent results, further DNS studies at higher Reynolds number are desirable in the future.

Acknowledgements

The authors wish to thank Geoffrey Lilley and Jay Hardin for useful discussions and their helpful comments on a preliminary draft of the manuscript.

References

D. G. Crighton, 'Basic Principles of Aerodynamic Noise Generation,' *Prog. Aerospace Sci.*, **16**, pp. 31-96 (1975).

D. G. Crighton, 'Computational Aeroacoustics for Low Mach Number Flows,' *Computational Aeroacoustics*, J. C. Hardin and M. Y. Hussaini, eds., pp. 50-68, Springer Verlag (1993)

G. Erlebacher, M. Y. Hussaini, H. O. Kreiss and S. Sarkar 'The Analysis and Simulation of Compressible Turbulence,' *Theor. and Comp. Fluid Dyn. 2*, 73-95 (1990).

J. E. Ffowcs Williams, 'Aeroacoustics,' Ann. Rev. Fluid Mech., **9**, pp. 447-468 (1977).

T. B. Gatski, 'Sound Production due to Large-Scale Coherent Structures,' *AIAA Paper 79-4081* (1979).

M. E. Goldstein, 'Aeroacoustics,' *NASA SP-346*, (1974).

J. O. Hinze, 'Turbulence,' McGraw-Hill (1975).

M. S. Howe, 'Contributions to the Theory of Aerodynamic Sound With Applications to Excess Jet Noise and the Theory of the Flute,' *J. Fluid Mech.*, **71**, pp. 625-673 (1975).

A. Leonard, 'Computing three-dimensional flows with vortex elements,' in *Annual Reviews of Fluid Mechanics*, **17**, pp. 523-559 (1985).

M. Lesieur, *Turbulence in Fluids*, 2nd edn., Kluwer Academic, (1990).

M. J. Lighthill, 'On Sound Generated Aerodynamically I. General Theory,' *Proc. Roy. Soc. A*, **211**, pp. 564-587 (1952).

M. J. Lighthill, 'On Sound Generated Aerodynamically II. Turbulence as a Source of Sound,' *Proc. Roy. Soc. A*, **222**, pp. 1-32 (1954)

M. J. Lighthill, 'The Final Panel Discussion,' *Computational Aeroacoustics*, J. C. Hardin and M. Y. Hussaini, eds., pp. 499-513, Springer Verlag (1993).

G. M. Lilley, 'On the Noise from Jets,' *AGARD-CP-131*, pp. 13.1-13.12 (1974).

G. M. Lilley, 'The Radiated Noise from Isotropic Turbulence Revisited,' *NASA CR-191547, ICASE Report No. 93-75.*

O. M. Phillips, 'On the Generation of Sound by Supersonic Shear Layers,' *J. Fluid Mech.*, **9**, pp. 1-28 (1960).

A. Powell, 'Theory of Vortex Sound,' *J. Acoust. Soc. America*, **36**, pp. 177-195 (1964).

I. Proudman, 'The Generation of Noise by Isotropic Turbulence,' *Proc. Roy. Soc. A*, **214**, pp. 119-132 (1952).

H. Ribner, 'The Generation of Sound by Turbulent Jets,' *Advances in Applied Mechanics*, **8**, H. L. Dryden and Th. von Karman, eds., pp. 103-182 (1964).

S. Sarkar, G. Erlebacher, M. Y. Hussaini, and H. O. Kreiss, 'The Analysis and Modelling of Dilatational Terms in Compressible Turbulence,' *J. Fluid Mech.*, **227**, 473 (1991a).

S. Sarkar, G. Erlebacher, and M. Y. Hussaini, 'Direct Simulation of Compressible Turbulence in a Shear Flow,' *Theor. Comput. Fluid Dyn.*, **2**, 291 (1991b).

S. Sarkar, 'The Pressure-Dilatation Correlation in Compressible Turbulence,' *Phys. Fluids A*, **4**, pp. 2674-2682(1992).

S. Sarkar and M. Y. Hussaini, " Computation of the Acoustic Radiation from Bounded Homogeneous Flows," *Computational Aeroacoustics*, J. C. Hardin and M. Y. Hussaini, eds., pp. 335-349, Springer Verlag (1993).

J. Seiner, 'Fluid Dynamics and Noise Emission Associated with Supersonic Jets,' *Studies in Turbulence*, T. B. Gatski, S. Sarkar and C. G. Speziale, eds., pp. 297-323 (1991).

A. Witkowska and D. Juve, 'Numerical Simulation of Noise Generated by Homogeneous and Isotropic Turbulence,' Proc. 13th Colloquium on Aero- and Hydro-Acoustics, Lyon, (1993).

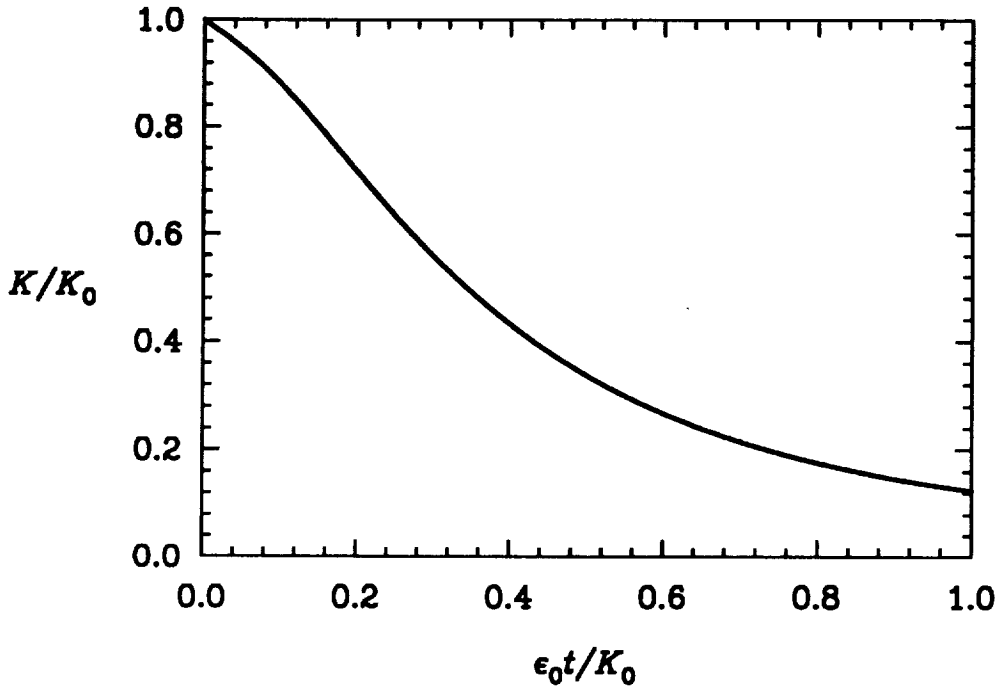

Fig. 1. Evolution of the turbulent kinetic energy in the DNS.

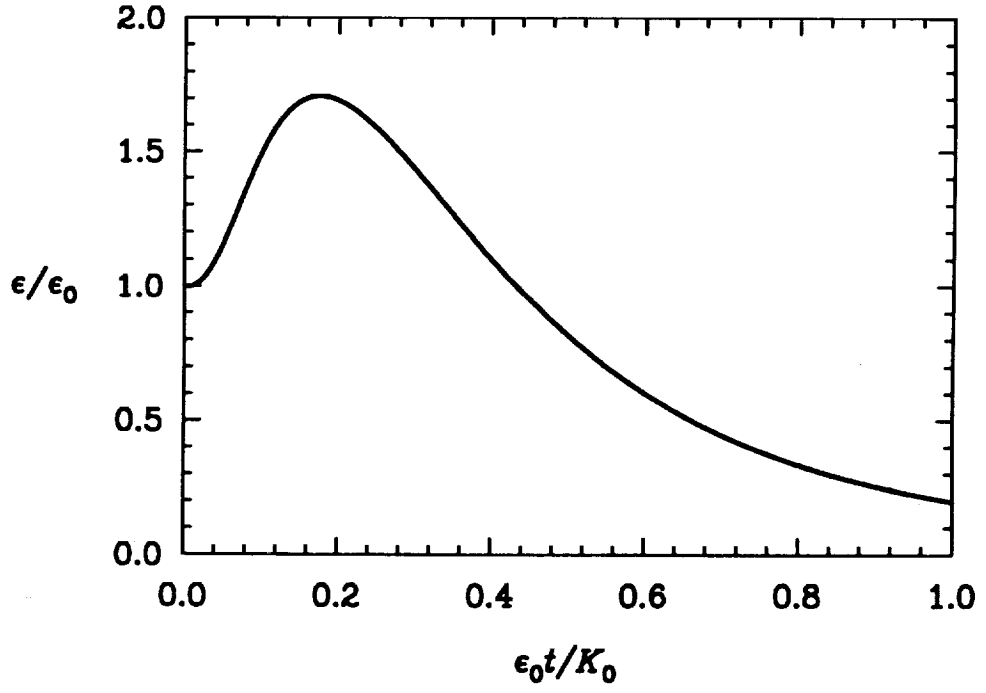

Fig. 2. Evolution of the turbulent dissipation rate in the DNS.

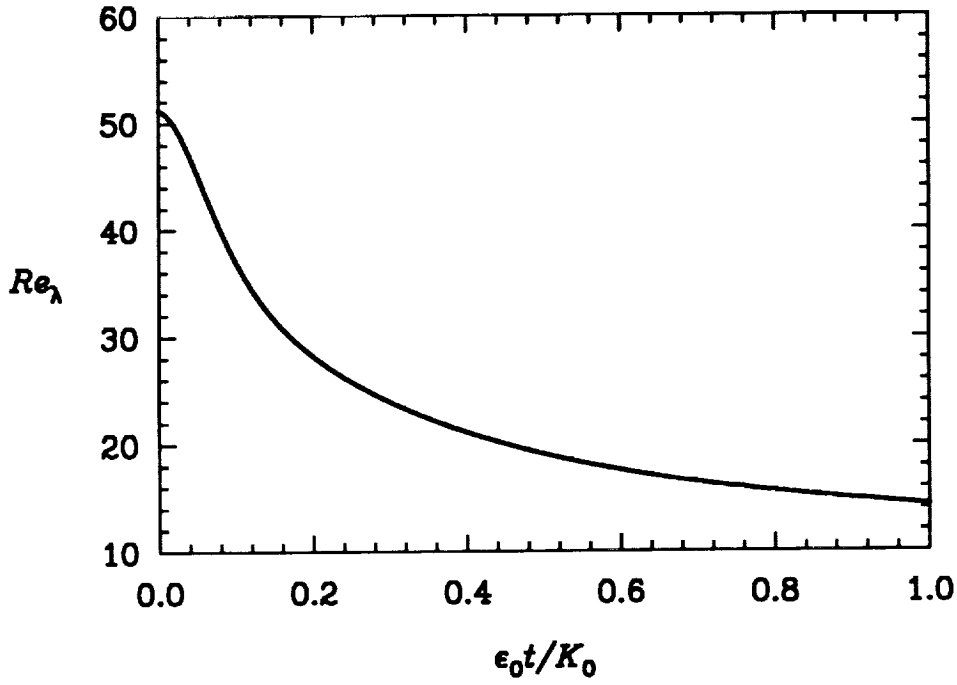

Fig. 3. Evolution of the microscale Reynolds number Re_λ in the DNS.

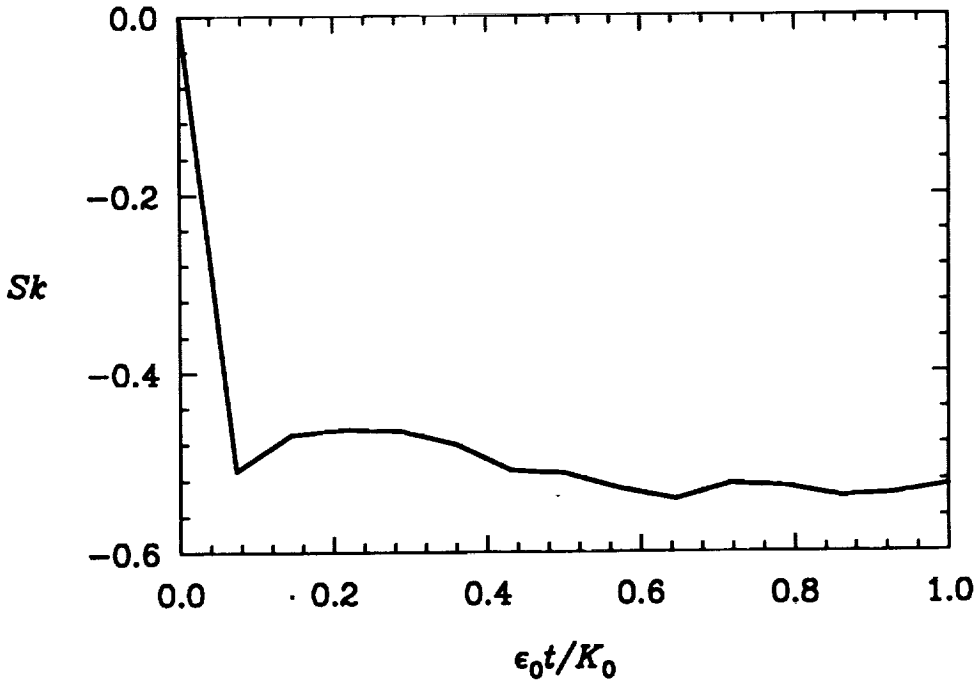

Fig. 4. Evolution of the velocity derivative skewness in the DNS.

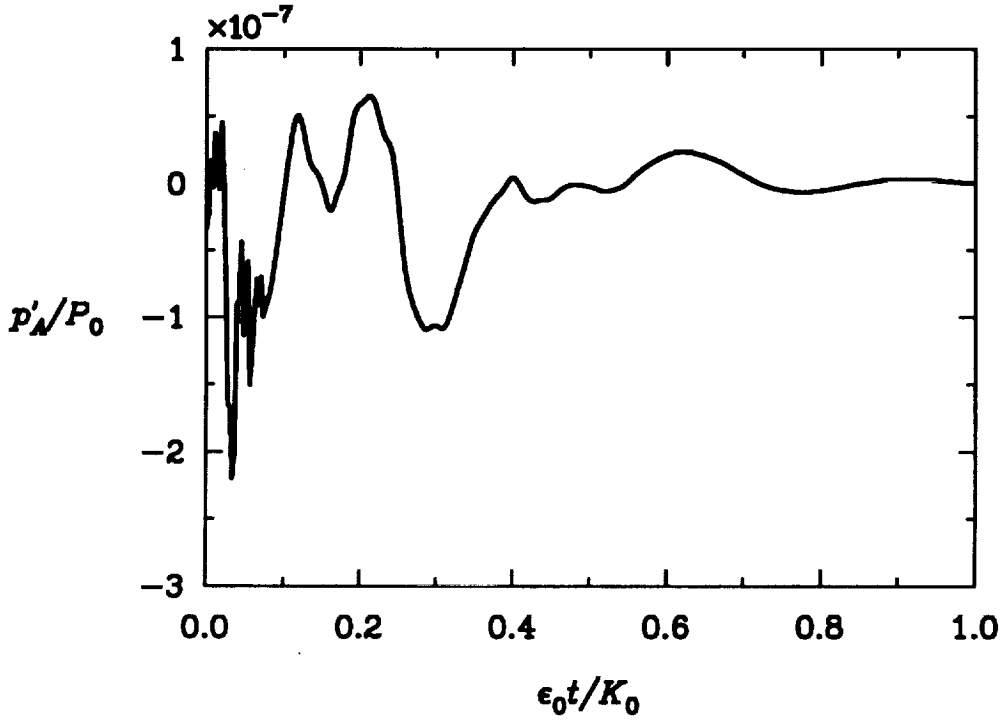

Fig. 5. Acoustic pressure at far–field point 1 in the DNS.

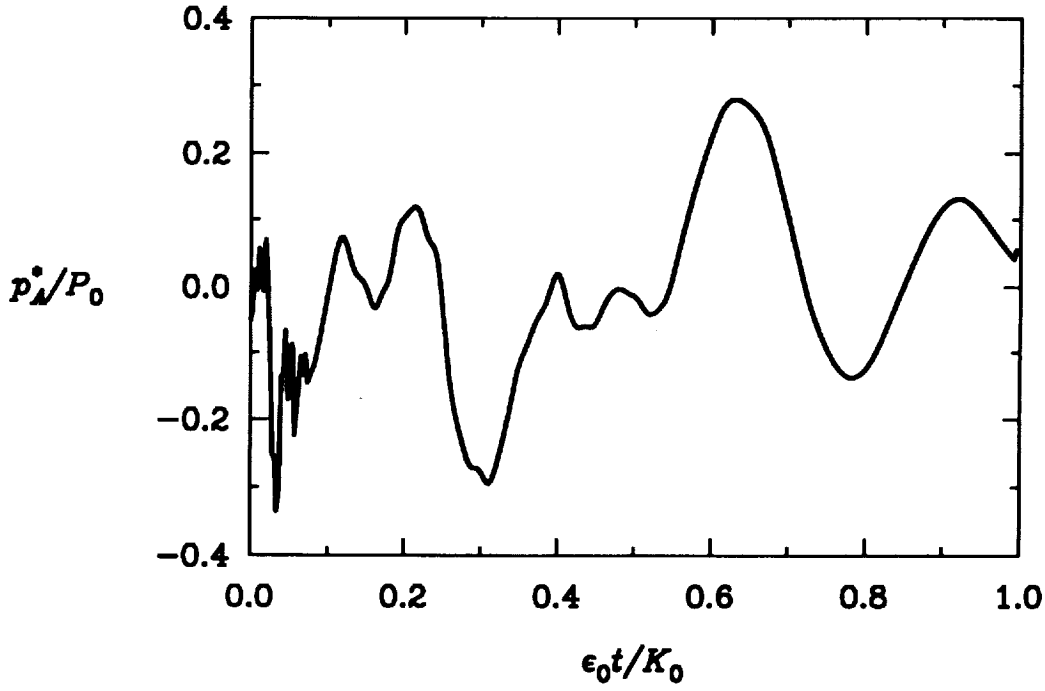

Fig. 6. Acoustic pressure at the far–field point scaled to remove the decay of turbulence.

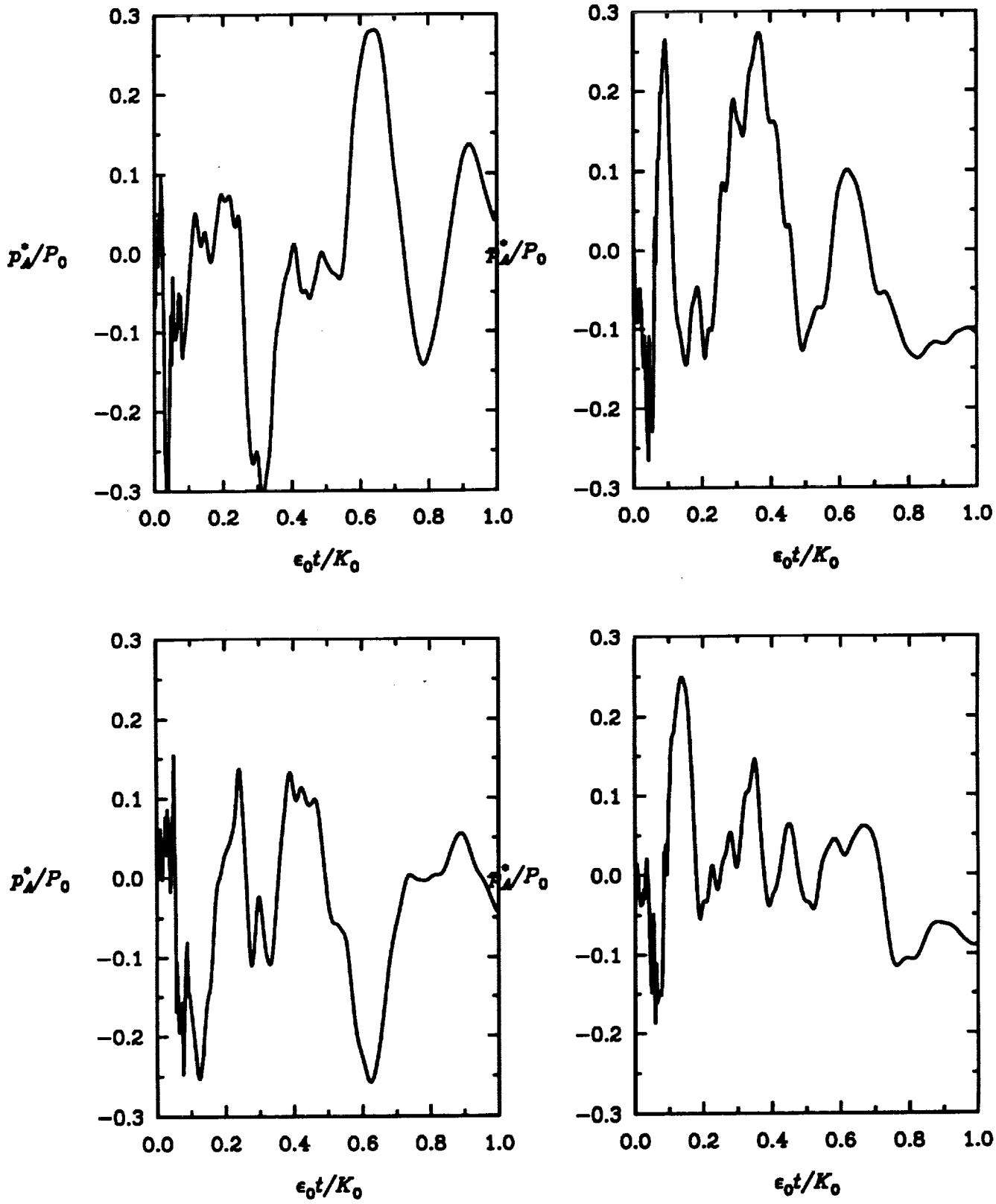

Fig. 7. Time series of the normalized acoustic pressure p_A^* at four observation points in the DNS.

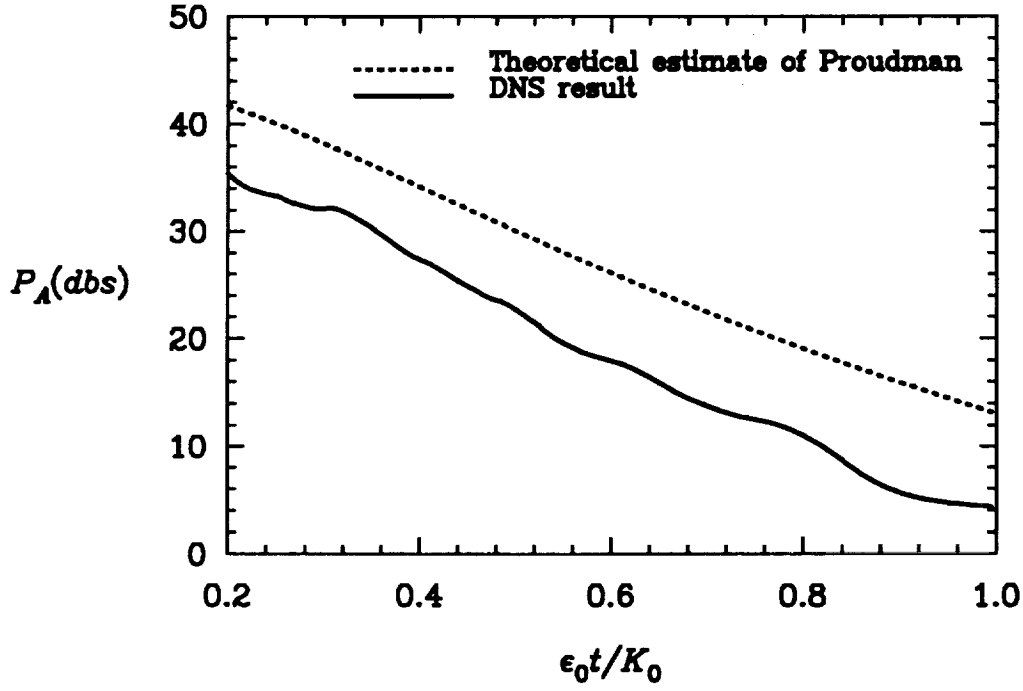

Fig. 8. The average power of the radiated sound.

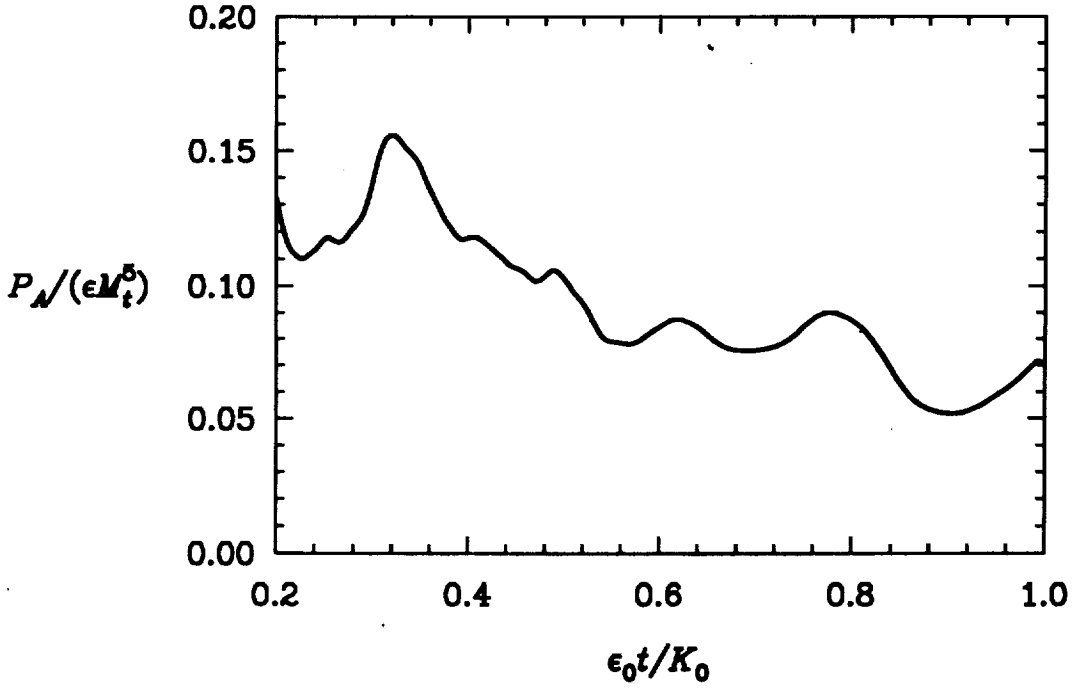

Fig. 9. The scaled acoustic power in the DNS.

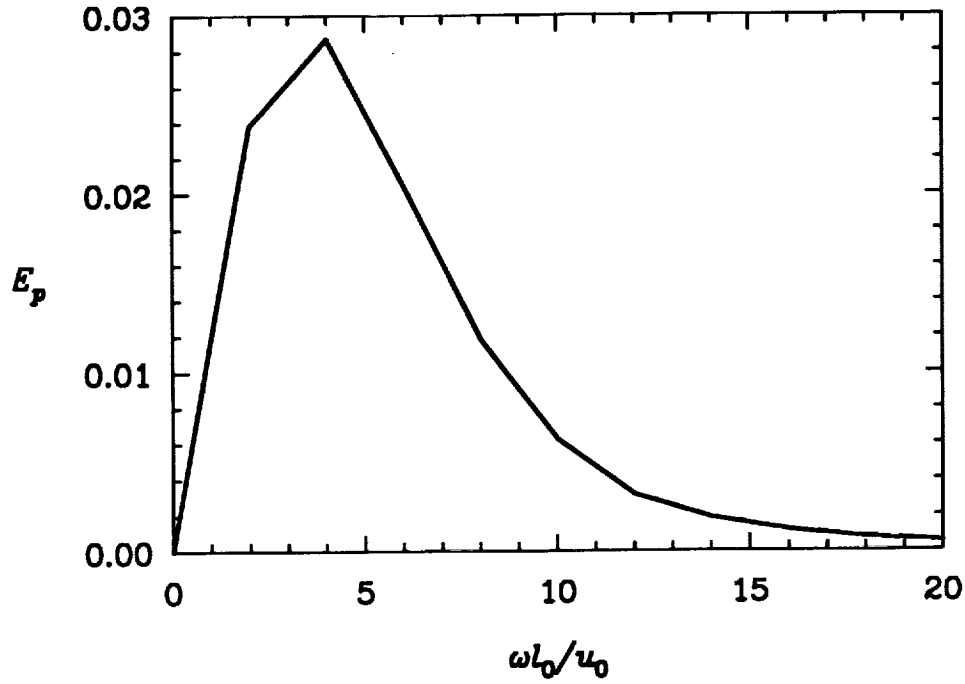

Fig. 10. The frequency spectrum of the computed acoustic pressure.

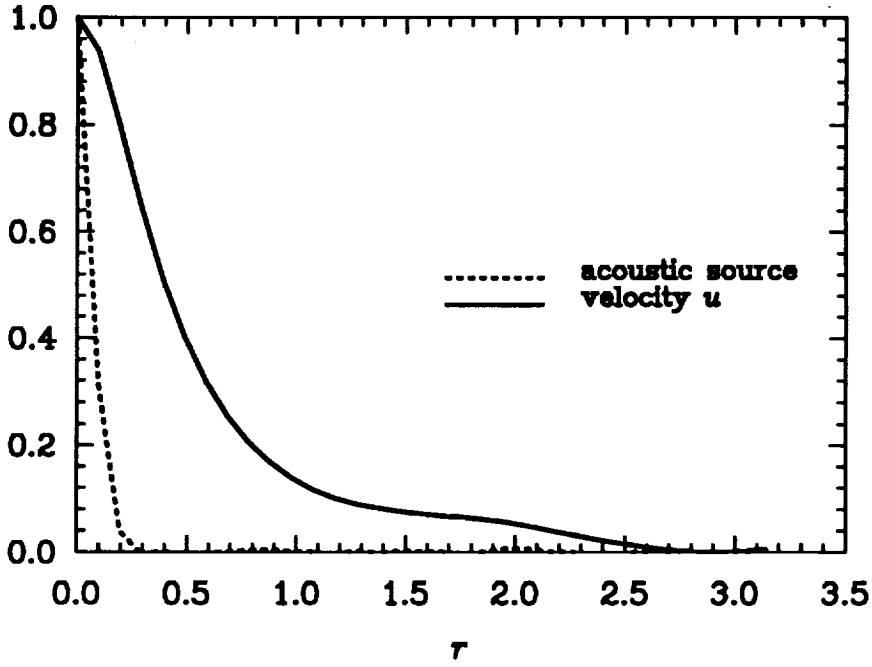

Fig. 11. DNS results at time $\epsilon_0 t/K_0$=0.7 on longitudinal spatial correlations.

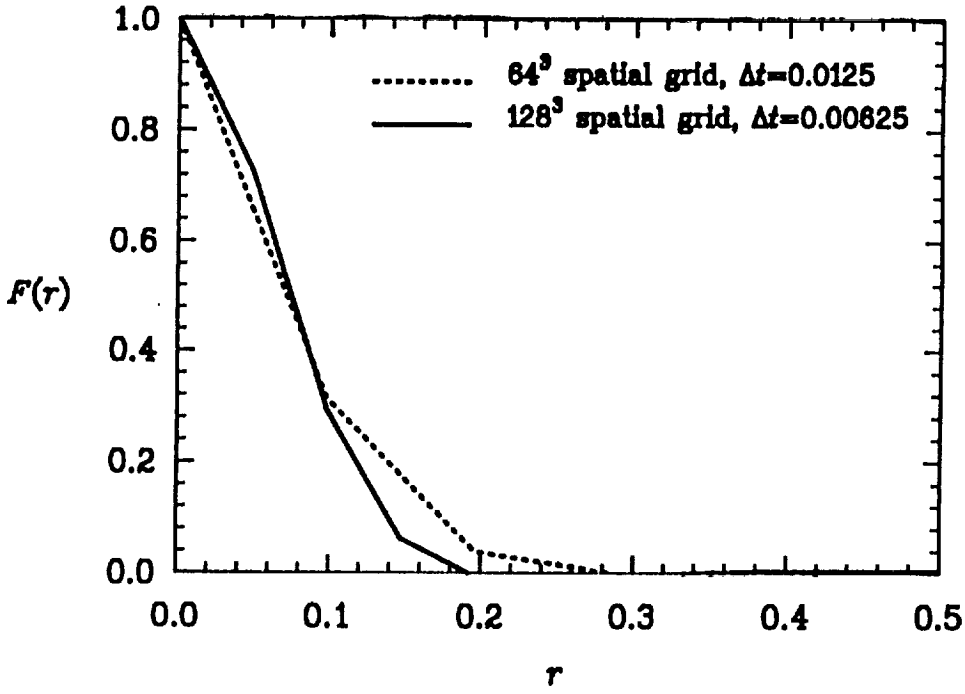

Fig. 12. Effect of increased spatial and temporal resolution on $F(r)$, the longitudinal spatial correlation of the acoustic source.

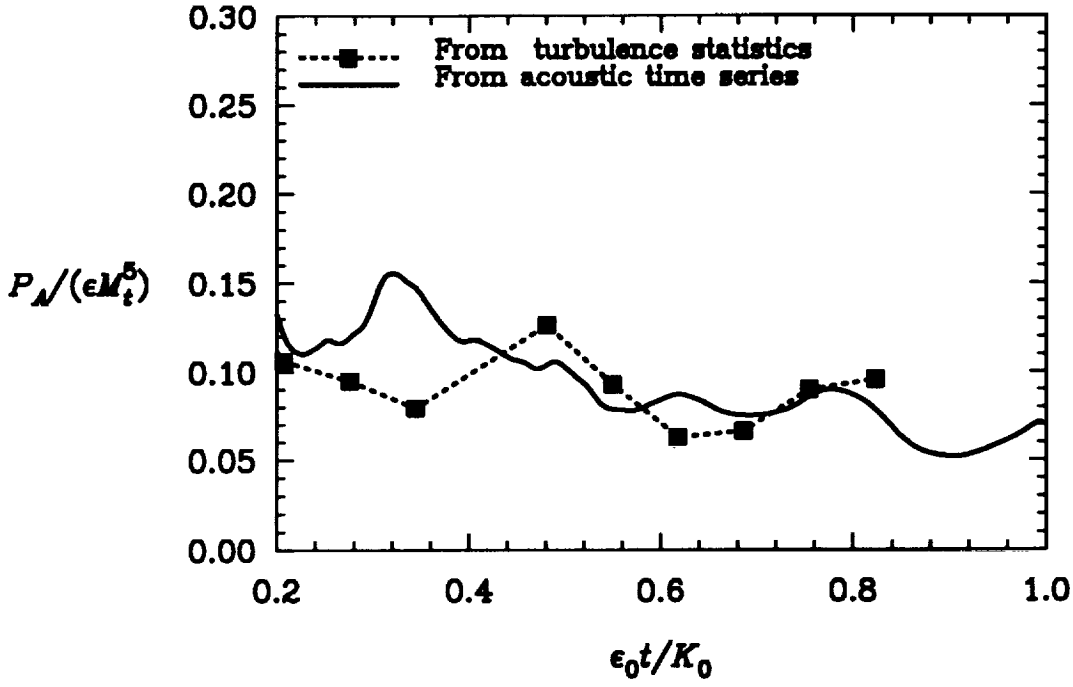

Fig. 13. Comparison of two methods of obtaining the scaled acoustic power. Solid line is an ensemble average from the computed acoustic pressure, and symbols are from the computed two–point correlation of $\bar{T}_{ij}$.

REPORT DOCUMENTATION PAGE

Form Approved
OMB No. 0704-0188

1. AGENCY USE ONLY *(Leave blank)*	2. REPORT DATE	3. REPORT TYPE AND DATES COVERED
	October 1993	Contractor Report

4. TITLE AND SUBTITLE
COMPUTATION OF THE SOUND GENERATED BY ISOTROPIC TURBULENCE

5. FUNDING NUMBERS
C NAS1-19480
WU 505-90-52-01

6. AUTHOR(S)
S. Sarkar
M. Y. Hussaini

7. PERFORMING ORGANIZATION NAME(S) AND ADDRESS(ES)
Institute for Computer Applications in Science and Engineering
Mail Stop 132C, NASA Langley Research Center
Hampton, VA 23681-0001

8. PERFORMING ORGANIZATION REPORT NUMBER
ICASE Report No. 93-74

9. SPONSORING/MONITORING AGENCY NAME(S) AND ADDRESS(ES)
National Aeronautics and Space Administration
Langley Research Center
Hampton, VA 23681-0001

10. SPONSORING/MONITORING AGENCY REPORT NUMBER
NASA CR-191543
ICASE Report No. 93-74

11. SUPPLEMENTARY NOTES
Langley Technical Monitor: Michael F. Card
Final Report
Submitted to Journal of Fluid Mechanics

12a. DISTRIBUTION/AVAILABILITY STATEMENT
Unclassified–Unlimited

Subject Category 34

12b. DISTRIBUTION CODE

13. ABSTRACT *(Maximum 200 words)*

The acoustic radiation from isotropic turbulence is computed numerically. A hybrid direct numerical simulation approach which combines direct numerical simulation (DNS) of the turbulent flow with the Lighthill acoustic analogy is utilized. It is demonstrated that the hybrid DNS method is a feasible approach to the computation of sound generated by turbulent flows. The acoustic efficiency in the simulation of isotropic turbulence appears to be substantially less than that in subsonic jet experiments. The dominant frequency of the computed acoustic pressure is found to be somewhat larger than the dominant frequency of the energy-containing scales of motion. The acoustic power in the simulations is proportional to ϵM_t^5 where ϵ is the turbulent dissipation rate and M_t is the turbulent Mach number. This is in agreement with the analytical result of Proudman (1952), but the constant of proportionality is smaller than the analytical result. Two different methods of computing the acoustic power from the DNS data bases yielded consistent results.

14. SUBJECT TERMS	15. NUMBER OF PAGES
computational aeroacoustics; turbulence	30
	16. PRICE CODE: A03

17. SECURITY CLASSIFICATION OF REPORT	18. SECURITY CLASSIFICATION OF THIS PAGE	19. SECURITY CLASSIFICATION OF ABSTRACT	20. LIMITATION OF ABSTRACT
Unclassified	Unclassified		

NSN 7540-01-280-5500

Standard Form 298(Rev. 2-89)
Prescribed by ANSI Std. Z39-18
298-102

☆U.S. GOVERNMENT PRINTING OFFICE: 1993 - 528-064/86087